



# Depletion of Pax7+ satellite cells does not affect diaphragm adaptations to running in young or aged mice

Kevin A. Murach, Amy L. Confides, Angel Ho, Janna R. Jackson, Lina S. Ghazala , Charlotte A. Peterson and Esther E. Dupont-Versteegden 

College of Health Sciences, Department of Rehabilitation Sciences, and the Center for Muscle Biology, University of Kentucky, Lexington, KY, USA

## Key points

- Satellite cell depletion does not affect diaphragm adaptations to voluntary wheel running in young or aged mice.
- Satellite cell depletion early in life (4 months of age) has minimal effect on diaphragm phenotype by old age (24 months).
- Prolonged satellite cell depletion in the diaphragm does not result in excessive extracellular matrix accumulation, in contrast to what has been reported in hind limb muscles.
- Up-regulation of Pax3 mRNA+ cells after satellite cell depletion in young and aged mice suggests that Pax3+ cells may compensate for a loss of Pax7+ satellite cells in the diaphragm.
- Future investigations should focus on the role of Pax3+ cells in the diaphragm during adaptation to exercise and ageing.

**Abstract** Satellite cell contribution to unstressed diaphragm is higher compared to hind limb muscles, which is probably attributable to constant activation of this muscle to drive ventilation. Whether satellite cell depletion negatively impacts diaphragm quantitative and qualitative characteristics under stressed conditions in young and aged mice is unknown. We therefore challenged the diaphragm with prolonged running activity in the presence and absence of Pax7+ satellite cells in young and aged mice using an inducible Pax7<sup>CreER</sup>-R26R<sup>DTA</sup> model. Mice were vehicle (Veh, satellite cell-replete) or tamoxifen (Tam, satellite cell-depleted) treated at 4 months of age and were then allowed to run voluntarily at 6 months (young) and 22 months (aged). Age-matched, cage-dwelling, Veh- and Tam-treated mice without wheel access served as activity controls. Diaphragm muscles were analysed from young (8 months) and aged (24 months) mice. Satellite cell depletion did not alter diaphragm mean fibre cross-sectional area, fibre type distribution or extracellular matrix content in young or aged mice, regardless of running activity. Resting *in vivo* diaphragm function was also unaffected by satellite cell depletion. Myonuclear density was maintained in young satellite cell-depleted mice regardless of running, although it was modestly reduced in aged sedentary (−7%) and running (−19%) mice without satellite cells ( $P < 0.05$ ). Using fluorescence *in situ* hybridization, we detected higher Pax3 mRNA+ cell density in both young and aged satellite cell-depleted diaphragm muscle ( $P < 0.05$ ), which may compensate for the loss of Pax7+ satellite cells.

(Received 9 May 2017; accepted after revision 18 July 2017; first published online 24 July 2017)

**Corresponding author** E. E. Dupont-Versteegden: College of Health Sciences, Department of Rehabilitation Sciences, and the Center for Muscle Biology, University of Kentucky, Room 210E Wethington Building, 900 South Limestone Street, Lexington, KY 40536, USA. Email: eedupo2@uky.edu

**Abbreviations** CSA, cross-sectional area; DAPI, 4',6-diaminidino-2-phenylindole; DTA, diphtheria toxin A; ECM, extracellular matrix; FISH, fluorescence *in situ* hybridization; MoM, mouse on mouse; MyHC, myosin heavy chain; Pax3, paired box 3; Pax7, paired box 7; PFA, paraformaldehyde; Tam, tamoxifen; TSA, tyramide signal amplification; UTR, untranslated region; Veh, vehicle; WGA, wheat germ agglutinin.

## Introduction

The diaphragm is arguably the most vital skeletal muscle. Distinct from other skeletal muscles, the diaphragm is primarily controlled involuntarily and is activated constantly to drive ventilation. To sustain this high level of activity, the diaphragm possesses a more oxidative and fatigue-resistant fibre type profile than locomotor skeletal muscles. Apart from these differences, the diaphragm is similar to all other skeletal muscles in that it may contract voluntarily (e.g. breath holding, deliberate hyperventilation, coughing) and can be subject to ageing-induced functional impairment (Gosselin *et al.* 1994; Tolep *et al.* 1995; Criswell *et al.* 1997, 2003a; Polkey *et al.* 1997; Greising *et al.* 2013). Moreover, inactivity compounds ageing-induced diaphragm dysfunction; aged diaphragm lacks the functional 'reserve' to recover from brief (12 h) mechanical ventilation (Criswell *et al.* 2003b). Failure of the diaphragm to contract normally results in decreased performance and, depending on the severity of dysfunction, could result in respiratory complications, a reduced quality of life, an inability to perform airway-clearing manoeuvres and death.

Satellite cells (Pax7+) are the predominant stem cell population in skeletal muscle. These cells are indispensable for regeneration following muscle injury (Lepper *et al.* 2011; McCarthy *et al.* 2011; Murphy *et al.* 2011; Sambasivan *et al.* 2011) and are suggested to be responsible for myonuclear replacement and accretion (Stockdale & Holtzer, 1961; Moss & Leblond, 1970; Moss & Leblond, 1971; Schiaffino *et al.* 1972; Carlson, 1973). Surprisingly, satellite cell depletion during adulthood in conditional Pax7 knockout mice does not exacerbate sarcopenia in locomotor skeletal muscles (Fry *et al.* 2015; Keefe *et al.* 2015), nor does it impair adaptations to wheel-run training (Jackson *et al.* 2015). However, the diaphragm experiences a greater satellite cell contribution to muscle fibres than hind limb muscles throughout the lifespan in sedentary mice (Keefe *et al.* 2015; Pawlikowski *et al.* 2015). These data suggest a high rate of myonuclear replacement and homeostatic remodelling in the diaphragm.

Insight into the contribution of satellite cells to diaphragm myofibres has only been acquired from sedentary, cage-dwelling mice under completely unstressed conditions (Keefe *et al.* 2015; Pawlikowski *et al.* 2015). There is no information regarding how satellite cell-depleted diaphragm muscle responds to common physiological stress. The present study aimed to challenge the diaphragm with prolonged voluntary wheel running activity in the presence and absence of satellite cells in young and old mice. Utilizing the inducible Pax7<sup>CreER</sup>-R26R<sup>DTA</sup> model, we treated mice at 4 months of age with vehicle (Veh) or tamoxifen (Tam), and then

allowed them to run voluntarily at 6 or 22 months of age. We hypothesized that satellite cell depletion via Tam-induced recombination before 2 months of running would negatively impact diaphragm adaptations to 2 months of running and cause an exacerbated effect in aged mice. By contrast to our hypothesis, we generally found that satellite cell depletion did not negatively impact quantitative or qualitative diaphragm adaptations to running in young or aged mice. However, Pax3 mRNA+ cell density was higher in the absence of satellite cells, indicating a potential compensatory mechanism for the loss of satellite cells in diaphragm muscle.

## Methods

### Ethical approval

All animal procedures were conducted in accordance with institutional guidelines for the care and use of laboratory animals and were approved by the Institutional Animal Care and Use Committee of the University of Kentucky, which operates under the guidelines of the Animal Welfare Act and the US Public Health Service Policy on the Humane Care and Use of Laboratory Animals. Mice were housed in a temperature and humidity-controlled room and maintained under a 14:10 h light/dark cycle with food and water *ad libitum*. Animals were killed via a lethal dosage of sodium pentobarbital (150 mg kg<sup>-1</sup>) injected i.p., followed by cervical dislocation.

### Animal model

The Pax7-DTA (Diphtheria toxin A) mouse is a genetic mouse model that allows for conditional and specific depletion of Pax7-expressing cells (satellite cells) upon Tam administration. The Pax7-DTA mouse was generated by crossing the Pax7<sup>CreER/CreER</sup> to the Rosa26<sup>DTA/DTA</sup>, as described previously (McCarthy *et al.* 2011).

### Experimental design

A diagram depicting the detailed animal protocol is shown in Fig. 1A. Adult female Pax7-DTA mice (4 months of age,  $n = 9-12$  per group) received either an i.p. injection of Tam at a dose of 2.5 mg day<sup>-1</sup> for five consecutive days, or were injected with a Veh control (15% ethanol in sunflower seed oil) as described previously (Jackson *et al.* 2015). A washout period of at least 8 weeks followed the injections. At 6 (young) and 22 (aged) months of age, Veh- or Tam-treated mice were singly housed and randomly divided into two groups: sedentary or wheel running. The running wheels were connected to a mechanical counter that recorded wheel rotations using ClockLab software (Actimetrics, Wilmette, IL, USA). The software analysed running speed (km h<sup>-1</sup>), total distance run (km day<sup>-1</sup>)

and total time run ( $\text{h day}^{-1}$ ). The animals had access to food and water *ad libitum* and were checked daily for health and wellness. Following an 8 week running period, the animals were killed and their diaphragm muscles were dissected, processed and stored at  $-80^{\circ}\text{C}$  for further analyses, as described below.

### Immunohistochemistry and image analysis

Immunohistochemical procedures were performed in accordance with previously published protocols (McCarthy *et al.* 2011; Fry *et al.* 2014a; Jackson *et al.* 2015). Diaphragm muscle was pinned to a cork block at resting length, covered with a thin layer of Tissue Tek OCT compound (Sakura Finetek, Torrance, CA, USA) and then quickly frozen in liquid nitrogen-cooled isopentane and stored at  $-80^{\circ}\text{C}$  until sectioning. Frozen muscles were sectioned at  $-23^{\circ}\text{C}$  ( $8\ \mu\text{m}$ ), air-dried and stored at  $-20^{\circ}\text{C}$ . For Pax7 staining, sections were fixed

in 4% paraformaldehyde (PFA), followed by epitope retrieval using sodium citrate (10 mM, pH 6.5) at  $92^{\circ}\text{C}$ . For both Pax7 and dystrophin staining, endogenous peroxidase activity was blocked with 3% hydrogen peroxide in PBS, followed by an additional blocking step with 1% Tyramide Signal Amplification (TSA) blocking reagent (TSA kit, T20935; Invitrogen, Carlsbad, CA, USA) and Mouse-on-Mouse blocking reagent (Vector Laboratories, Burlingame, CA, USA). Pax7 primary antibody (dilution 1:100; Developmental Studies Hybridoma Bank, Iowa City, IA, USA) or dystrophin primary antibody (dilution 1:100, VPD505; Vector Laboratories) were diluted in 1% TSA blocking buffer and applied overnight. Samples were then incubated with anti-mouse biotin-conjugated secondary antibody (dilution 1:1000, 115-065-205; Jackson ImmunoResearch, West Grove, PA, USA), followed by streptavidin-HRP (dilution 1:500, S-911; Invitrogen). TSA AlexaFluor 488 (dystrophin) or 594 (Pax7) was used to visualize

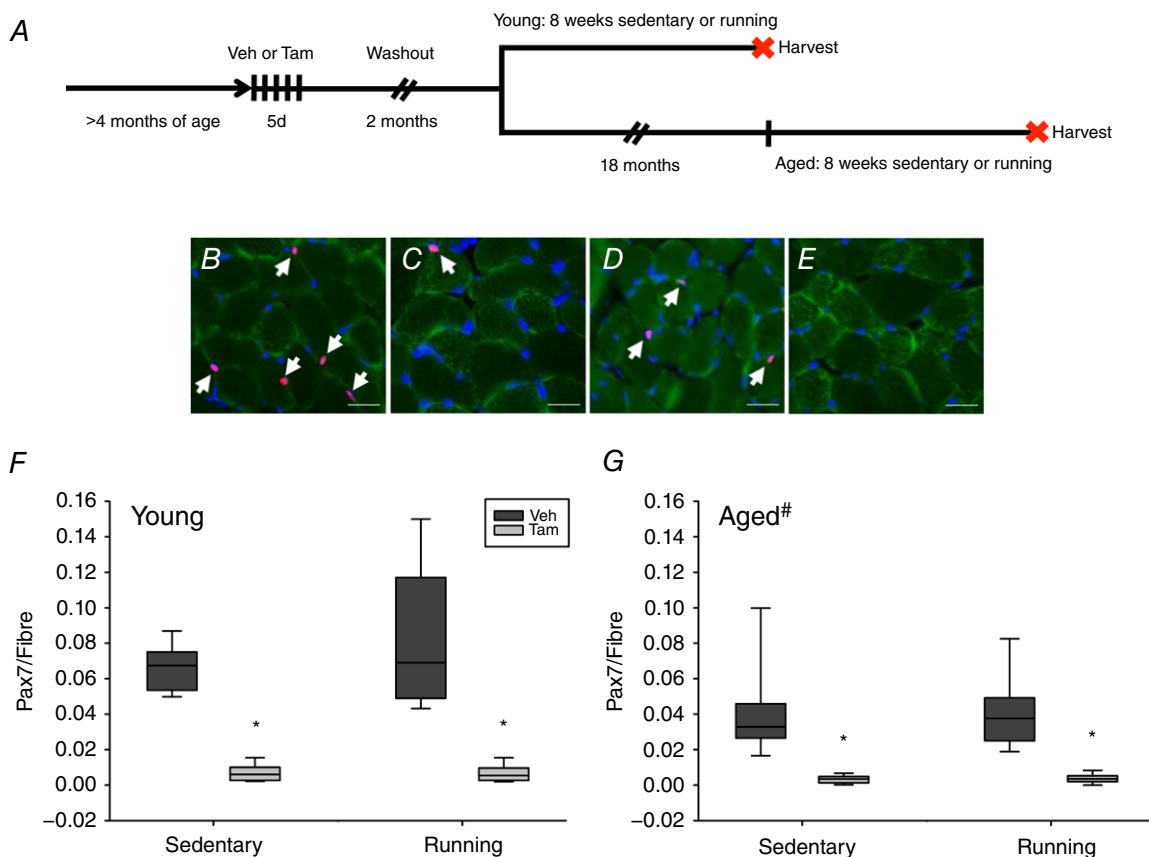


**Figure 1. Conditional depletion of satellite cells in young and aged mice**

A, study design schematic demonstrating the duration of Veh and Tam treatment, washout and running in young and aged mice. B–E, representative immunohistochemistry images of Pax7 staining in young (B) Veh- and (C) Tam-treated sedentary mice, and aged (D) Veh- and (E) Tam-treated sedentary mice. F, satellite cell density in young sedentary ( $n = 7$  Veh,  $n = 7$  Tam) and running ( $n = 7$  Veh,  $n = 10$  Tam) mice. G, satellite cell density in aged sedentary ( $n = 10$  Veh,  $n = 12$  Tam) and running ( $n = 9$  Veh,  $n = 11$  Tam) mice. Values are minimum, first quartile, median, third quartile and maximum; #main effect for age; \*main effect for satellite cell depletion ( $P < 0.05$ ).

antibody-binding. Sections were mounted and nuclei were stained with Vectashield Antifade mounting media with 4',6-diaminidino-2-phenylindole (DAPI) (H1200; Vector Laboratories). Images were captured at 20 $\times$  magnification at room temperature using an upright fluorescence microscope (AxioImager M1; Zeiss, Oberkochen, Germany). Satellite cells identified as Pax7+/DAPI+ were counted by a blinded trained technician and normalized to fibre number to determine satellite cell density. Fibre borders were traced manually by a blinded trained technician to quantify fibre cross-sectional area (CSA). Myonuclear number from at least 50 fibres (Mackey *et al.* 2009) was counted by a blinded technician as DAPI+ nuclei within the dystrophin border (Fry *et al.* 2014a) and expressed per average fibre CSA.

Extracellular matrix content was measured by detection of *N*-acetyl-D-glucosamine using Texas Red-conjugated wheat germ agglutinin (WGA) (dilution 1:50, W21405; Invitrogen). Sections were fixed in 4% PFA, then incubated with WGA conjugate and images were captured at 20 $\times$  magnification. Staining was quantified using the thresholding feature in AxioVision Rel software (Zeiss). The area occupied by WGA was expressed relative to muscle fibre number. To evaluate fibre-type distribution, antibodies specific to myosin heavy chains type I, IIa and IIx, along with laminin, were applied. Frozen sections were incubated overnight with isotype specific anti-mouse secondary antibodies for MyHC I (dilution 1:75, IgG2B, BA.D5), MyHC IIa (neat, IgG1, SC.71) and MyHC IIx (neat, IgM, 6H1) from the Developmental Studies Hybridoma Bank, along with laminin (dilution 1:100, L9393; Sigma-Aldrich, St Louis, MO, USA). Sections were then incubated with secondary antibodies (dilution 1:250, goat anti-mouse IgG2b Alexa fluor 647, #A21242; dilution 1:500, IgG1 Alexa fluor 488, #A21121; dilution 1:250, IgM Alexa fluor 555, #A21426; all from Invitrogen), all diluted in PBS, along with the secondary antibody for laminin (dilution 1:150, IgG AMCA, CI-1000; Vector Laboratories). Sections were mounted with VectaShield (H1000; Vector Laboratories) and images were captured at 20 $\times$  magnification. Fibre type distribution was quantified manually by a blinded trained technician as percentage MyHC I, IIa, IIx and IIb (no staining).

### Single muscle fibre myonuclear analysis

After careful removal of a section of costal diaphragm, diaphragm muscle was left on the ribs, pinned down and fixed at resting length in 4% PFA for 48 h. Single fibres were isolated using a method described previously (Brack *et al.* 2005; McCarthy *et al.* 2011). Briefly, following a 2 h 40% NaOH digestion, single fibres were mechanically teased apart, strained and washed with PBS before being stained with DAPI (dilution 1:10,000 in PBS, D35471; Invitrogen)

for myonuclear visualization, with the assumption that most satellite cells were dissociated from the muscle fibres during the isolation steps. Nuclei that appeared to be loosely associated with the muscle fibre were not counted. Suspended fibres were dispersed onto a slide and mounted with Vectashield fluorescence mounting media (Vector Laboratories). Images were captured as z-stacks at 20 $\times$  magnification, and all fibres and nuclear measurements were made using AxioVision Rel software. Twenty fibres from each animal were measured by a blinded trained technician to determine the number of myonuclei per defined fibre segment.

### Fluorescence *in situ* hybridization (FISH) for Pax3 determination

High-fidelity antibodies for Pax3 protein identification on frozen muscle cross-sections are not readily available. To detect Pax3 cells in the diaphragm, we modified a version of the Stellaris RNA FISH protocol from Biosearch Technologies (Petaluma, CA, USA), using Stellaris RNA FISH Hybridization Buffer and Stellaris RNA FISH Wash Buffer A. RNA FISH probes were designed by Integrated DNA Technologies (Coralville, IA, USA) and labelled with a biotin tag. Diaphragm muscle was sectioned (8  $\mu$ m) and immediately fixed and stored in 100% ethanol at -20°C. Slides were rinsed and any RNases were inactivated by incubating in 0.1% (v/v) diethyl pyrocarbonate. This step also increases the sensitivity of the mRNA detection (Zimmerman *et al.* 2013). Samples were immersed in 4% PFA, washed in PBS and then incubated in Wash Buffer A for 5 min. Probes were added to the Hybridization Buffer to a concentration of 625 nM and then incubated on the slides for 5 h at 37°C in a humidified chamber. Following incubation with probes, samples were washed in Wash Buffer A and then incubated with streptavidin-HRP (Invitrogen). TSA AlexaFluor 594 (dilution 1:100; Invitrogen) was used to visualize staining. Sections were mounted and nuclei stained using Vectashield Antifade mounting media with DAPI (Vector Laboratories). The probes used were Pax3-1728, Pax3-3130 and NC (a negative control scramble probe):

```
Pax3-
1728
/5Biosg/mUmAmUmAmGmGmUmGmGmGmGmGmGm
GmAmCmAmAmUmAmG
3130
/5Biosg/mCmCmUmCmUmAmCmAmUmCmAmUm
AmCmCmCmUmUmCmC
NC (negative control)
/5Biosg/mGmCmGmAmCmUmAmUmAmCmGmCm
GmCmAmAmUmAmUmG
```

Pax3+ cells were identified as Pax3+/DAPI+ and were expressed per muscle fibre number.

**Table 1. Running performance in young and aged Veh- and Tam-treated mice**

	Young		Aged <sup>#</sup>	
	Veh	Tam	Veh	Tam
Distance (km)	13.3 ± 0.5	9.2 ± 1.2*	7.9 ± 1.3	5.8 ± 1.5*
Time run (h)	10.2 ± 0.3	8.5 ± 0.7*	8.0 ± 1.1	6.2 ± 1.2*
Speed (km h <sup>-1</sup> )	1.28 ± 0.03	1.04 ± 0.06	0.96 ± 0.10	0.85 ± 0.14

\*Significantly different from Veh. <sup>#</sup>Main effect for age. *n* = 4–7 per group

### Ultrasound analysis of *in vivo* diaphragm function in conscious mice

Ultrasound was performed in a blinded fashion on mice when they were awake and held in an upright position. Although these measures may not produce a true 'resting' value because there was a probable adrenergic response from handling, this approach is more translatable than conducting these measures when the mouse was anaesthetized. The day before the scan, abdominal hair was removed with depilatory cream (Nair™ Church & Dwight Co., Trenton, NJ, USA). The probe with ultrasonic gel was placed on the abdomen close to the xyphoid process pointing upward for diaphragm visualization using the VisualSonics Vevo<sup>®</sup> 2100 Imaging System with MS-400 scan head (FujiFilm VisualSonics Inc., Toronto, ON, Canada) at 38 MHz. M-mode images were captured of 10–50 respiratory cycles. Of those, 10–20 cycles were measured for breath rate, breath depth, and inspiration and expiration velocity.

### Statistical analysis

Data were analysed with SigmaPlot software (Systat Software, San Jose, CA, USA). Data were checked for normality and those that were not normally distributed underwent a log transformation. Parametric analyses were used for all measures. To include all mice in the analysis, three-way ANOVAs were used to determine main effects for age, followed by a two-way ANOVA to test for effect of satellite cell depletion and running activity. If a significant effect or interaction was detected, an appropriate *post hoc* analysis was employed to determine the source of the significance. *P* ≤ 0.05 was considered statistically significant. Normally distributed data are reported as the mean ± SE, and non-normally distributed data are presented as minimum, first quartile, median, third quartile and maximum.

## Results

### Diaphragm satellite cell density is affected by age but not by running

Satellite cell density in the diaphragm is decreased with age, such that, in ambulatory Veh-treated controls, there was a

48% decrease in the aged (main effect for age, *P* < 0.05) (Fig. 1B–G). Consistent with previous findings in hind-limb muscles, satellite cell density was reduced by ≥ 90% with Tam administration in both young and aged mice and also remained depleted even after 18 months (McCarthy *et al.* 2011; Jackson *et al.* 2012, 2015; Fry *et al.* 2014a, 2015; Lee *et al.* 2015; Kirby *et al.* 2016; Murach *et al.* 2017). Regardless of Veh or Tam treatment, satellite cell density did not change with running in young or old mice (Fig. 1B–G).

### Running capacity is reduced with age and satellite cell depletion

Running speed (km h<sup>-1</sup>), time (h day<sup>-1</sup>) and distance (km day<sup>-1</sup>) were reduced in aged vs. young mice (*P* < 0.05) (Table 1). Consistent with previous findings from our laboratory (Jackson *et al.* 2015), satellite cell depletion negatively impacted running capacity in young mice, such that running time and distance were 16% and 30% lower, respectively, in satellite cell-depleted mice (Table 1). This effect was also present in aged mice, where running time and distance were 26% and 23% lower, respectively, in satellite cell-depleted mice (*P* < 0.05) (Table 1). We showed previously that reduced running is not attributable to a toxic effect of Tam and/or Cre expression since Tam-treated parental strain mice demonstrated normal running activity (Jackson *et al.* 2015).

### Myonuclear density is unaffected by age and running but is reduced in aged satellite cell-depleted diaphragm

Myonuclear density in isolated diaphragm single fibres (nuclei per fibre length) was not different between young and aged diaphragm (Fig. 2), indicating that myonuclear density is not decreased with age in diaphragm. Satellite cell depletion or running did not change myonuclear density measured on single fibres in young mice (Fig. 2A). Myonuclear density on single fibres was slightly lower in aged Tam-treated mice (−7% in ambulatory and −19% in runners), which was a consequence of the modest increase in myonuclear density observed with running in Veh-treated mice (+14%, *P* < 0.05) (Fig. 2B). Myonuclei per area measured on histological cross-sections was not

different between young and aged but did increase with running in young mice ( $P < 0.05$ ), which can probably be attributed to the fast-to-slow fibre type transition and the prevalence of smaller MyHC I fibres (Fig. 2C). Myonuclei per area did not change with satellite cell depletion or running in aged mice (Fig. 2D).

### Running-induced changes in diaphragm muscle are not affected by satellite cell depletion

Diaphragm muscle fibre CSA was not different between young and aged (Fig. 3). In young mice, muscle fibre CSA was reduced by running (−11% and −16% in Veh and Tam mice, respectively,  $P < 0.05$ ), although satellite cell depletion did not induce a difference (Fig. 3A). Running did not change fibre CSA in aged mice, nor did satellite cell depletion affect CSA in aged mice (Fig. 3B). Reduced muscle fibre CSA in young runners was probably accounted for by a fast-to-slower fibre type transition; the percentage of MHC IIX was decreased in young

runners, whereas MyHC I proportion increased ( $P < 0.05$ ) (Fig. 4A). A comparatively less-pronounced fast-to-slower fibre type transition was observed in aged runners, such that MyHC IIX was reduced and MyHC IIA was higher ( $P < 0.05$ ) (Fig. 4B). Satellite cell depletion had no effect on fibre type distribution in young compared to aged sedentary mice and changes in fibre type in response to running were not affected by satellite cell depletion (Fig. 4A and B). A representative immunohistochemistry image visualizing MyHC I, IIA and IIX is shown in Fig. 4C. Because the proportion of pure MyHC IIB was  $< 1\%$  in all diaphragm muscles, these fibres were not included in the analysis.

### Extracellular matrix is not affected by age, satellite cell depletion or running

We did not observe differences in extracellular matrix content between young and aged in the diaphragm (Fig. 5A and B), in contrast to what we have reported

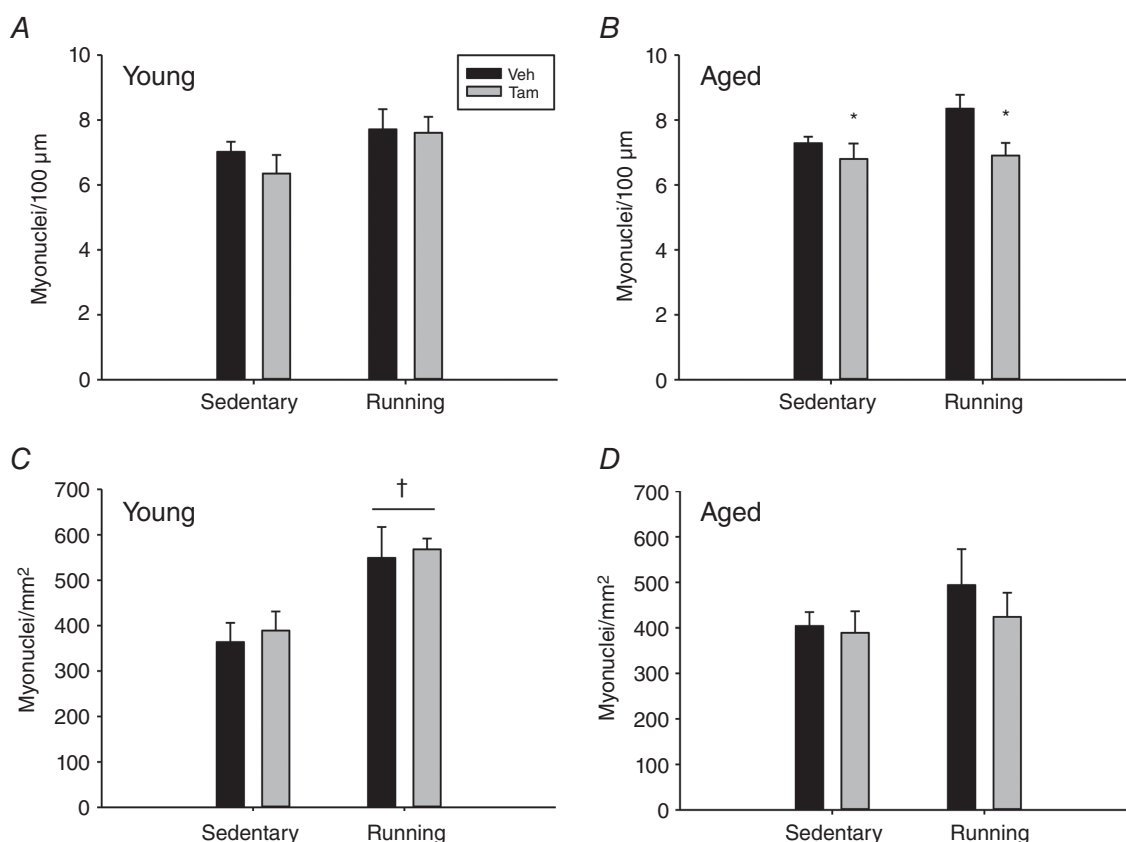


**Figure 2. Diaphragm myonuclear density in young and aged sedentary and running mice in the presence (Veh) and absence (Tam) of satellite cells**

A, single muscle fibre myonuclear density in young sedentary ( $n = 7$  Veh,  $n = 6$  Tam) and running ( $n = 8$  Veh,  $n = 7$  Tam) mice. B, single muscle fibre myonuclear density in aged sedentary ( $n = 7$  Veh,  $n = 7$  Tam) and running ( $n = 8$  Veh,  $n = 9$  Tam) mice. C, myonuclei per area from histological cross-sections in young sedentary ( $n = 4$  Veh,  $n = 5$  Tam) and running ( $n = 4$  Veh,  $n = 4$  Tam) mice. D, myonuclei per area from histological cross-sections in aged sedentary ( $n = 4$  Veh,  $n = 5$  Tam) and running ( $n = 4$  Veh,  $n = 5$  Tam) mice. Values are the mean  $\pm$  SE; \*main effect for satellite cell depletion ( $P < 0.05$ ); †main effect for running ( $P < 0.05$ ).

in hindlimb muscles (Fry *et al.* 2015; Lee *et al.* 2015). In addition, neither satellite cell depletion, nor running affected extracellular matrix content in young and aged mice.

### **In vivo diaphragm function is affected by running but not by satellite cell depletion or age**

To address diaphragm function in the conscious mouse, we used ultrasound imaging as shown on a representative tracing (Fig. 6A). No age-related differences were observed in breath depth (Fig. 6B), breathing rate, inspiration velocity or expiration velocity (Table 2). Breath depth was increased by running in young (35%) and aged (23%) mice ( $P < 0.05$ ) (Fig. 6B and C) and satellite cell depletion did not affect this increase ( $P < 0.05$ ) (Fig. 6B and C). Breathing rate, inspiration velocity and expiration velocity were not affected by running or satellite cell depletion in young or old mice ( $P > 0.05$ ) (Table 2).

### **Pax3 mRNA+ cells are elevated in satellite cell-depleted diaphragms**

To investigate whether another stem cell type in the diaphragm is affected by satellite cell depletion, we measured the density of Pax3 mRNA+ cells using FISH (Fig. 7A). We utilized two probe sets to detect Pax3: a general probe that identified all Pax3 transcripts (probe 1728) and one that included a miR-206 binding site in the 3' untranslated region (UTR) of the Pax3 mRNA that is not present in the diaphragm (probe 3130) (Boutet *et al.* 2012). Pax3 mRNA, as detected by probe 1728, is presumably not targeted for degradation by miR-206 in the diaphragm and is most probably translated into functional protein. Probe 1728 was readily detectable in the diaphragm (Fig. 7A), whereas NC probe (Fig. 7B)

and probe 3130 (not shown) were not observed in the diaphragm. Probe 1728 was also observed in the liver (positive control) (Fig. 7C) (Tsukamoto *et al.* 1994) but did not appear in the spleen (negative control) (Fig. 7D). The number of Pax3 mRNA+ cells (probe 1728) was not different between young and aged (Fig. 7E and F). However, Pax3 mRNA+ cells increased in young and aged satellite cell-depleted mice regardless of running status ( $P < 0.05$ ) (Fig. 7E and F), suggesting that these cells may compensate for the loss of Pax7+ cells.

## **Discussion**

The primary objective of the present study was to determine whether satellite cell depletion affects diaphragm adaptations to voluntary wheel running in young and aged mice. Because the diaphragm is the most active skeletal muscle, we hypothesized that satellite cell depletion would negatively impact diaphragm function and morphology when subjected to a physiological stressor, and that aged mice would suffer greater impairments than young mice. By contrast to our hypothesis, satellite cell depletion did not negatively affect functional or morphological adaptations to running in young or aged mice. Prolonged satellite cell depletion also did not affect muscle fibre size or fibrosis with ageing in the diaphragm. Interestingly, Pax3 mRNA+ cells increased in the absence of satellite cells in both young and aged sedentary and running mice. These findings challenge the presumed necessity of Pax7+ satellite cells for diaphragm maintenance in stressed and aged conditions and also provide insight into a potential compensatory mechanism for the loss of satellite cells.

Consistent with that reported previously in locomotor skeletal muscles utilizing the Pax7<sup>CreER</sup>-R26R<sup>DTA</sup> mouse model (McCarthy *et al.* 2011; Jackson *et al.* 2012, 2015;

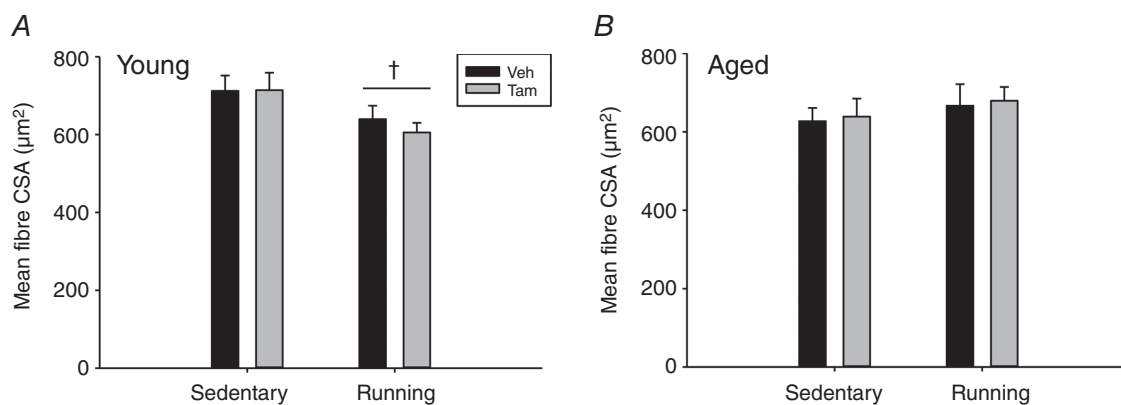


**Figure 3. Diaphragm muscle fibre CSA in young and aged sedentary and running mice in the presence (Veh) and absence (Tam) of satellite cells**

A, muscle fibre CSA in young sedentary ( $n = 7$  Veh,  $n = 8$  Tam) and running ( $n = 7$ ,  $n = 10$ ) mice. B, muscle fibre CSA in aged sedentary ( $n = 7$  Veh,  $n = 9$  Tam) and running ( $n = 9$  Veh,  $n = 10$  Tam) mice. Values are the mean  $\pm$  SE; †main effect for running ( $P < 0.05$ ).

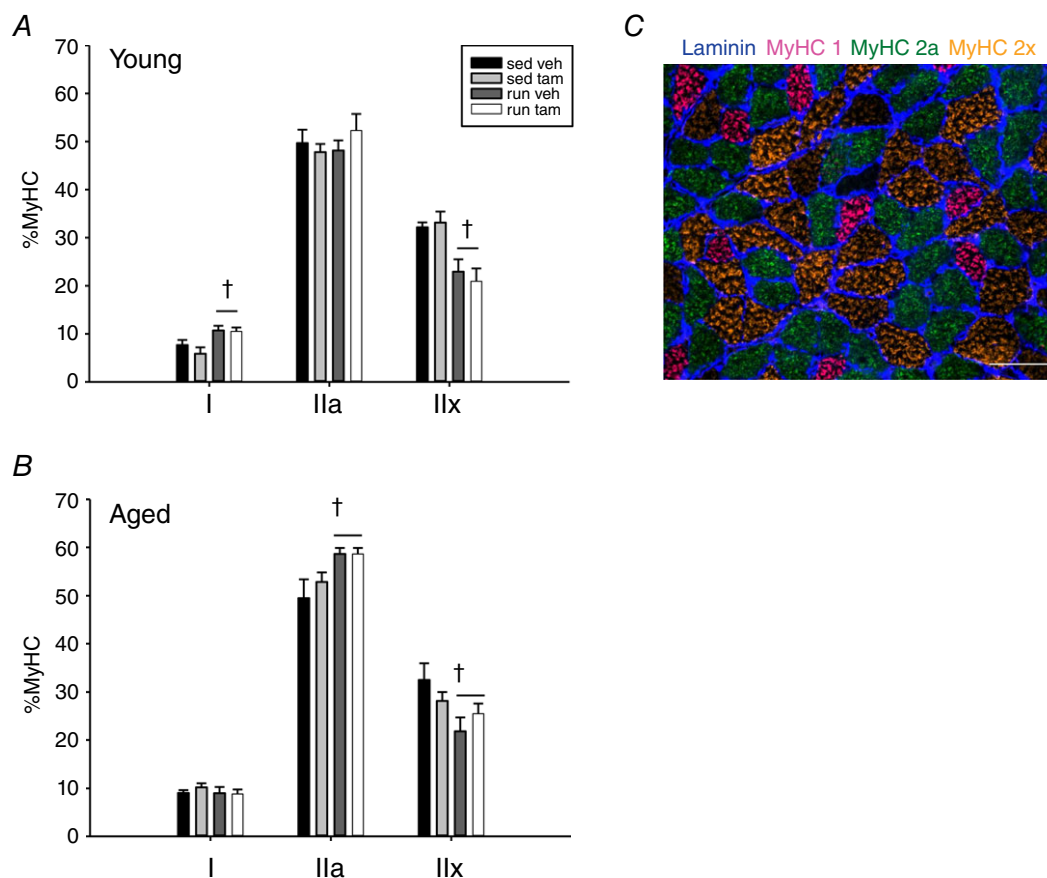
**Table 2.** *In vivo* diaphragm function in sedentary and running Veh- and Tam-treated mice

	Young				Aged			
	Veh		Tam		Veh		Tam	
	Sedentary	Running	Sedentary	Running	Sedentary	Running	Sedentary	Running
Breathing rate (breaths $\text{minute}^{-1}$ )	234 $\pm$ 22	270 $\pm$ 45	308 $\pm$ 32	247 $\pm$ 48	212 $\pm$ 19	209 $\pm$ 11	255 $\pm$ 43	231 $\pm$ 12
Inspiration velocity ( $\text{mm s}^{-1}$ )	11.1 $\pm$ 0.9	8.8 $\pm$ 1.0	10.0 $\pm$ 0.7	10.8 $\pm$ 4.0	10.1 $\pm$ 0.7	10.7 $\pm$ 1.3	9.4 $\pm$ 0.9	11.2 $\pm$ 0.9
Expiration velocity ( $\text{mm s}^{-1}$ )	12.1 $\pm$ 1.3	10.1 $\pm$ 1.1	10.3 $\pm$ 0.9	12.7 $\pm$ 2.3	10.9 $\pm$ 1.3	11.2 $\pm$ 1.5	11.0 $\pm$ 1.8	12.9 $\pm$ 1.6

*n* = 3–7 per group.

Fry *et al.* 2014a, 2015, 2017; Lee *et al.* 2015; Kirby *et al.* 2016; Murach *et al.* 2017), we achieved > 90% satellite cell depletion in the diaphragm after Tam administration. As expected, satellite cell depletion reduced running capacity in both young and aged mice. Muscle spindle morphology

and function is impaired in limb skeletal muscles in the absence of satellite cells, subsequently resulting in decreased coordination and reduced running performance (Jackson *et al.* 2015). Satellite cell depletion in young and aged mice had no effect on diaphragm muscle fibre size,

**Figure 4.** Diaphragm muscle fibre type distribution in young and aged sedentary and running mice in the presence (Veh) and absence (Tam) of satellite cells

*A*, muscle fibre type distribution in young sedentary (*n* = 6 Veh, *n* = 5 Tam) and running (*n* = 6 Veh, *n* = 9 Tam) mice. *B*, muscle fibre type distribution in aged sedentary (*n* = 6 Veh, *n* = 7 Tam) and running (*n* = 5 Veh, *n* = 6 Tam) mice. *C*, representative diaphragm immunohistochemistry image visualizing MyHC type I (pink), Ila (green) and Ilx (orange); scale bar = 50  $\mu\text{m}$ . Values are the mean  $\pm$  SE; \*different from Tam within aged runners; †main effect for running ( $P < 0.05$ ).



MyHC type distribution, extracellular matrix content or resting/nominally stressed *in vivo* functional adaptations to running. Although we cannot preclude that satellite cell depletion affects diaphragm function when running, or that the difference in running activity influenced the findings, we propose that reduced running performance following satellite cell depletion is primarily mediated by perturbations to intrafusal fibres in limb skeletal muscles, and not diaphragm dysfunction (Jackson *et al.* 2015).

Satellite cell-mediated adaptations to running were not highly anticipated, even in satellite cell-replete mice (i.e. increased Pax7+ cell number, myonuclear density or fibre size); however, it was still unexpected that diaphragm adaptation to running without satellite cells was uncompromised. Two laboratories agree that the diaphragm experiences a relatively high degree of satellite cell contribution to muscle fibres in sedentary cage-dwelling mice, although there are discrepancies in the observed frequency (Keefe *et al.* 2015; Pawlikowski *et al.* 2015). Pawlikowski *et al.* (2015) report 80% of diaphragm muscle fibres experience a satellite cell fusion event during a 2 week chase period in reporter mice (relative to 20% in hindlimb muscles). Keefe *et al.* (2015) report that 18% of diaphragm fibres experience satellite cell fusion after a 6 month chase, although labelling continues at the highest rate in diaphragm relative to other skeletal muscles as age progresses. The diaphragm is constantly activated to

drive ventilation and, congruent with the notion that muscle oxidative potential may impact the requirement for satellite cells during remodelling (Bagley, 2014; Fry *et al.* 2014b; Murach *et al.* 2016), the findings of Keefe *et al.* (2015) and Pawlikowski *et al.* (2015) suggest that the highly oxidative diaphragm muscle undergoes frequent satellite cell-mediated myonuclear turnover to maintain homeostasis. This interpretation is not consistent with our finding that, regardless of running, young mice do not lose myonuclei with more than 2 months of satellite cell depletion in the presence of maintained fibre size. On the other hand, aged sedentary and running mice did experience slight but significant reductions in myonuclear density following 20 months of satellite cell depletion (−7% and −19% in isolated single muscle fibres, respectively, with similar albeit not statistically significant trends on cross-sections) without myofibre atrophy. It is conceivable that fewer myonuclei in aged diaphragms may cause dysfunction in very old age (> 24 months), which may be addressed in future investigations. To reconcile the disconnect between reporter mouse and satellite cell-depleted mouse observations, we hypothesized that another stem cell population may compensate to maintain diaphragm myonuclear density in the absence of satellite cells.

Pax3 is a transcription factor expressed in the dorsal neural tube and somite of the developing embryo, and is

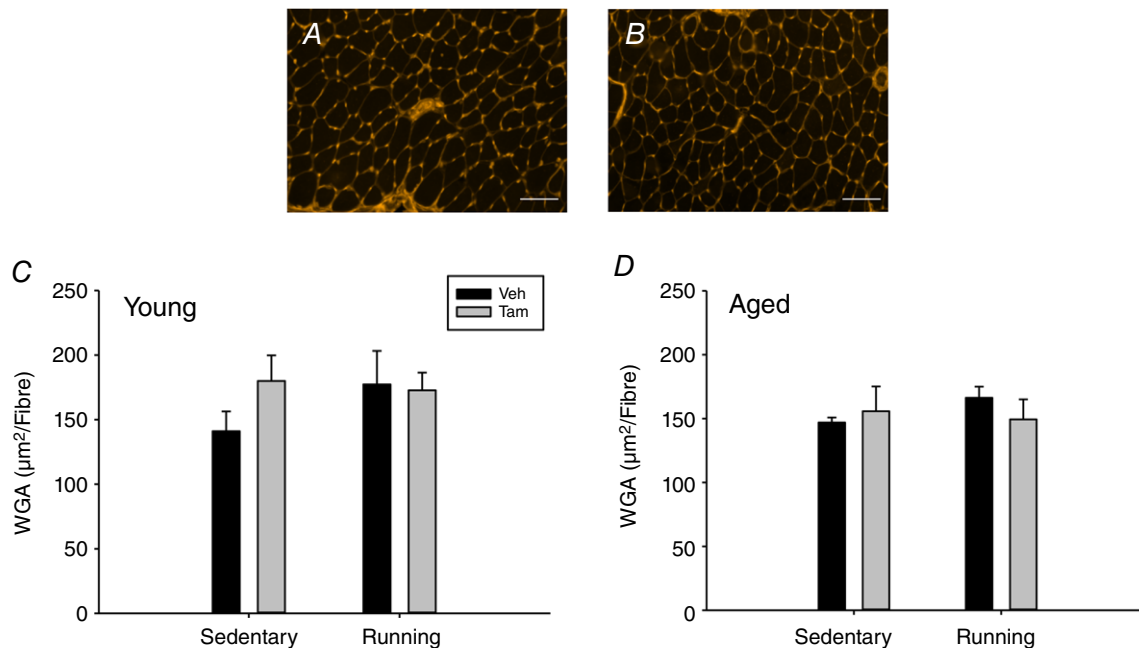


**Figure 5. Diaphragm extracellular matrix content (ECM) in young and aged sedentary and running mice in the presence (Veh) and absence (Tam) of satellite cells**

Representative muscle cross-section visualizing WGA from (A) young and (B) aged diaphragm muscle; scale bar = 50 µm. C, ECM content in young sedentary ( $n = 7$  Veh,  $n = 8$  Tam) and running ( $n = 7$  Veh,  $n = 9$  Tam) mice. D, ECM content in young sedentary ( $n = 7$  Veh,  $n = 10$  Tam) and running ( $n = 6$  Veh,  $n = 8$  Tam) mice.

a paralogue to Pax7 (Kuang *et al.* 2006; Relaix *et al.* 2006). Quiescent Pax3+ satellite cells are generally not prominent in limb skeletal muscles, although they are more abundant in the diaphragm (Montarras *et al.* 2005; Relaix *et al.* 2006). As a result of alternative polyadenylation processing, Pax3 transcript in the diaphragm contains a truncated 3' UTR that lacks a miR-206 binding site. Without this binding site, Pax3 protein is expressed preferentially in the diaphragm muscles (Boutet *et al.* 2012; Pasut & Rudnicki, 2012). The roles of Pax3+ muscle stem cells in adult skeletal muscle are still being defined, although it is clear that Pax3+ cells are a distinct population that can adopt functions of Pax7+ satellite cells (Montarras *et al.* 2005). Because a reliable Pax3 antibody is not available, we used fluorescence *in situ* hybridization on frozen diaphragm cross-sections to identify Pax3-expressing cells. Independent of age and running, we found that Pax3 mRNA+ cells were robustly up-regulated in the absence of satellite cells in the diaphragm. A probe designed to include the miR-206 binding site was not visualized in the diaphragm, suggesting that the Pax3 mRNA detected in the diaphragm is most probably translated into a functional

protein. It is conceivable that this unique muscle-specific stem cell population may replace absent Pax7+ cells in young mice, supporting myonuclear turnover and partially preventing myonuclear loss in aged mice.

Depletion of satellite cells in early adulthood does not result in a deleterious phenotype by ~6 months (Cheung *et al.* 2012; Keefe *et al.* 2015) or 20–24 months of age (Fry *et al.* 2015; Keefe *et al.* 2015) in limb skeletal muscles of mice. These recent findings challenge the pervasive belief that satellite cell attrition and/or dysfunction during ageing mediates sarcopenia (Conboy *et al.* 2005; Shefer *et al.* 2006; Snijders *et al.* 2009). Only one investigation has explored the effects of satellite cell depletion during aging in the diaphragm (Keefe *et al.* 2015). At 20 months of age, lifelong satellite cell-depleted diaphragm muscles resemble those that aged with a full complement of satellite cells (Keefe *et al.* 2015). Our findings extend the work of Keefe *et al.* (2015): more prolonged satellite cell depletion (20 vs. 14 months) into older age (24 vs. 20 months) with or without running does not cause muscle fibre atrophy or an otherwise abnormal diaphragm phenotype, despite modest reductions in myonuclear density. Our

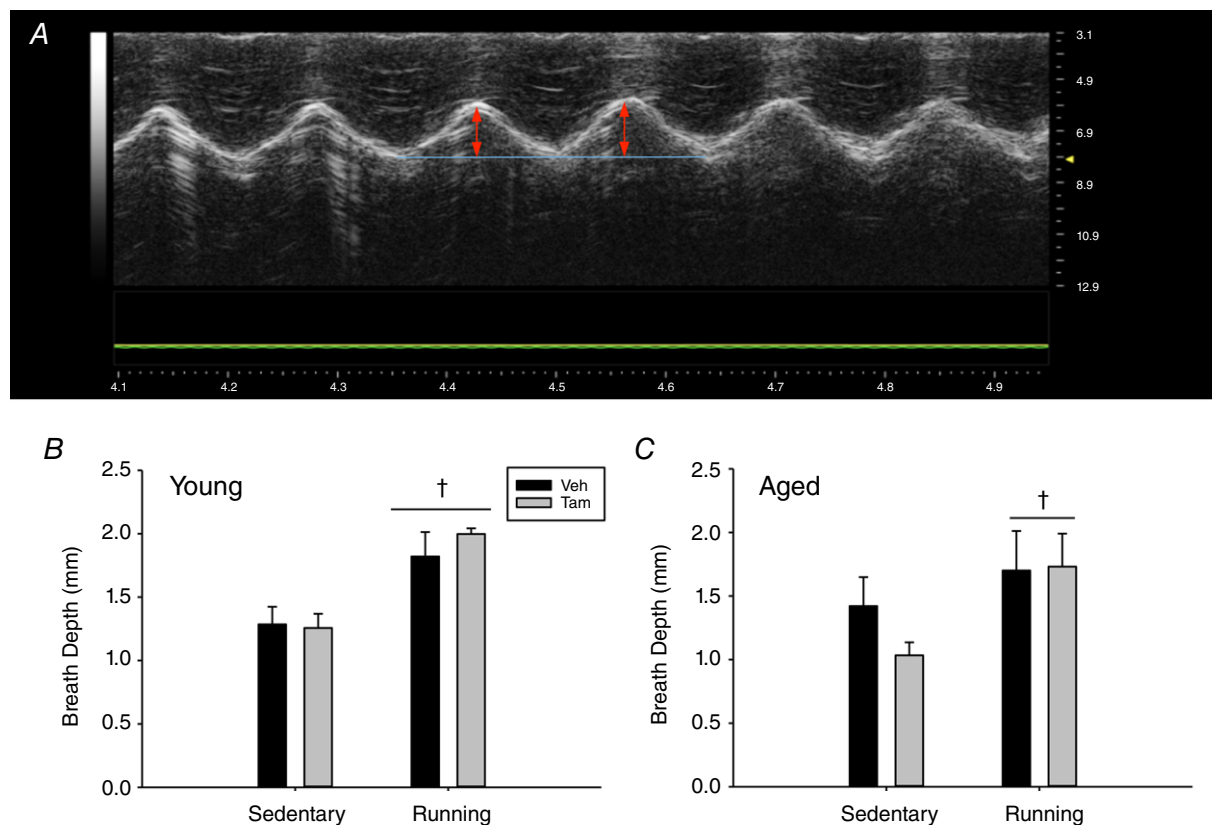


**Figure 6.** *In vivo* diaphragm breath depth at rest in young and aged sedentary and running mice in the presence (Veh) and absence (Tam) of satellite cells

A, representative ultrasound tracing of diaphragm excursion. Arrows show the magnitude of inspiration and expiration. B, breath depth in young sedentary ( $n = 5$  Veh,  $n = 4$  Tam) and running ( $n = 3$  Veh,  $n = 4$  Tam) mice. C, breath depth in aged sedentary ( $n = 7$  Veh,  $n = 4$  Tam) and running ( $n = 6$  Veh,  $n = 6$  Tam) mice. Values are the mean  $\pm$  SE; †main effect for running ( $P < 0.05$ ). [Colour figure can be viewed at [wileyonlinelibrary.com](http://wileyonlinelibrary.com)]

findings are also consistent with those of Keefe *et al.* (2015) regarding the general effects of age on the diaphragm. Satellite cell number in Veh-treated mice declined, whereas fibre size and fibre type distribution were largely unaffected. By contrast to what is observed in limb skeletal muscles (Fry *et al.* 2015, Lee *et al.* 2015), pronounced extracellular matrix deposition does not manifest in the ageing diaphragm, nor is fibrosis exacerbated by the loss of satellite cells. In concert with maintained muscle fibre size, a lack of fibrosis may explain preserved resting *in vivo* diaphragm function with ageing. Because Pax7+ satellite cells play a central role in regulating extracellular matrix remodelling (Murphy *et al.* 2011; Fry *et al.* 2014a, 2015, 2017; Liu *et al.* 2015; Southard *et al.* 2016), it is attractive to speculate that the increased prevalence of Pax3 mRNA+ cells in the satellite cell-depleted diaphragm may account

for the lack of fibrosis in aged mice. It is also conceivable that constant activity in the diaphragm throughout the lifespan is somehow protective against fibrotic deposition regardless of the presence of satellite cells. Collectively, these data suggest that the ageing process is distinct in the diaphragm.

In summary, satellite cells are not imperative to globally maintain diaphragm quantitative or qualitative characteristics in response to running and/or ageing. We report a modest reduction in myonuclear density in aged mice following satellite cell depletion, although this did not result in diaphragm muscle fibre atrophy or impaired *in vivo* function at rest. An increased prevalence of Pax3 mRNA+ cells in the diaphragm of young and old satellite cell-depleted mice may compensate for the loss of Pax7+ satellite cells, although more work is

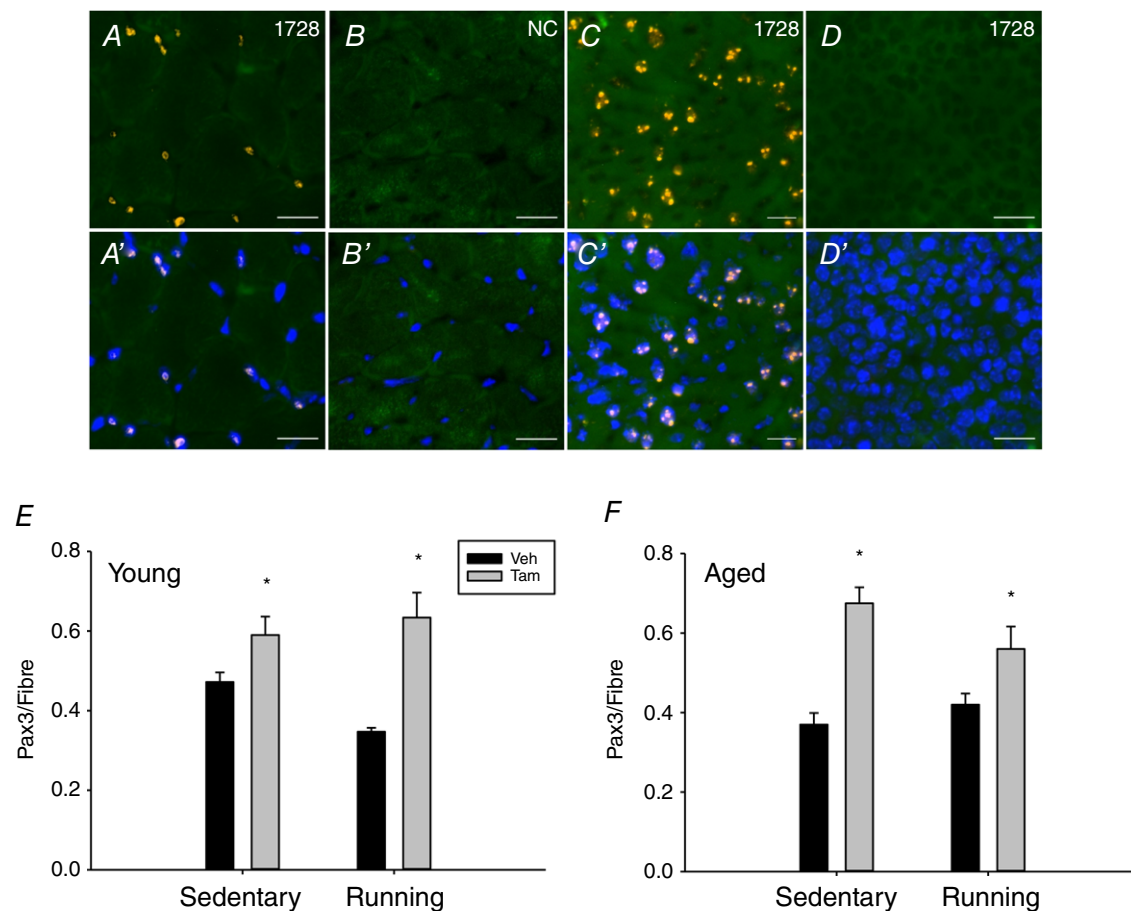


**Figure 7. Diaphragm Pax3 mRNA+ cells in young and aged sedentary and running mice in the presence (Veh) and absence (Tam) of satellite cells**

A and A', representative images of Pax3 mRNA+ cells (orange) overlapping with DAPI+ myonuclei (blue) in the diaphragm. B and B', lack of Pax3 mRNA+ cells in the diaphragm using a scrambled probe (NC). C and C', representative images of Pax3 mRNA+ cells overlapping with DAPI+ myonuclei in liver tissue (probe 1728, positive control). D and D', only DAPI+ myonuclei in spleen tissue, indicating a lack of Pax3 mRNA+ cells (probe 1728, negative control); scale bars = 20  $\mu$ m. E, Pax3+ cell density in young sedentary ( $n = 6$  Veh,  $n = 6$  Tam) and running ( $n = 5$  Veh,  $n = 8$  Tam) mice. F, Pax3+ cell density in mature sedentary ( $n = 6$  Veh,  $n = 7$  Tam) and running ( $n = 6$  Veh,  $n = 7$  Tam) mice. Values are the mean  $\pm$  SE; \*main effect for satellite cell depletion ( $P < 0.05$ ).

needed to define the role of Pax3+ cells in the diaphragm. The findings reported in the present study challenge our original hypothesis but highlight that the unique structure and function of the diaphragm may require adaptive mechanisms that are not present in other skeletal muscles.

## References

- Bagley JR (2014). Fibre type-specific hypertrophy mechanisms in human skeletal muscle: potential role of myonuclear addition. *J Physiol* **592**, 5147–5148.
- Boutet SC, Cheung TH, Quach NL, Liu L, Prescott SL, Edalati A, Iori K & Rando TA (2012). Alternative polyadenylation mediates microRNA regulation of muscle stem cell function. *Cell Stem Cell* **10**, 327–336.
- Brack AS, Bildsoe H & Hughes SM (2005). Evidence that satellite cell decrement contributes to preferential decline in nuclear number from large fibres during murine age-related muscle atrophy. *J Cell Sci* **118**, 4813–4821.
- Carlson BM (1973). The regeneration of skeletal muscle. A review. *Am J Anat* **137**, 119–149.
- Cheung TH, Quach NL, Charville GW, Liu L, Park L, Edalati A, Yoo B, Hoang P & Rando TA (2012). Maintenance of muscle stem-cell quiescence by microRNA-489. *Nature* **482**, 524–528.
- Conboy IM, Conboy MJ, Wagers AJ, Girma ER, Weissman IL & Rando TA (2005). Rejuvenation of aged progenitor cells by exposure to a young systemic environment. *Nature* **433**, 760–764.
- Criswell DS, Powers SK, Herb RA & Dodd SL (1997). Mechanism of specific force deficit in the senescent rat diaphragm. *Respir Physiol* **107**, 149–155.
- Criswell DS, Shanely RA, Betters JJ, McKenzie MJ, Sellman JE, Van Gammeren DL & Powers SK (2003a). Cumulative effects of aging and mechanical ventilation on in vitro diaphragm function. *Chest J* **124**, 2302–2308.
- Criswell DS, Shanely RA, Betters JJ, McKenzie MJ, Sellman JE, Van Gammeren DL & Powers SK (2003b). Cumulative effects of aging and mechanical ventilation on in vitro diaphragm function. *Chest J* **124**, 2302–2308.
- Fry CS, Kirby TJ, Kosmac K, McCarthy JJ & Peterson CA (2017). Myogenic progenitor cells control extracellular matrix production by fibroblasts during skeletal muscle hypertrophy. *Cell Stem Cell* **20**, 56–69.
- Fry CS, Lee JD, Jackson JR, Kirby TJ, Stasko SA, Liu H, Dupont-Versteegden EE, McCarthy JJ & Peterson CA (2014a). Regulation of the muscle fiber microenvironment by activated satellite cells during hypertrophy. *FASEB J* **28**, 1654–1665.
- Fry CS, Lee JD, Mula J, Kirby TJ, Jackson JR, Liu F, Yang L, Mendias CL, Dupont-Versteegden EE, McCarthy JJ & Peterson CA (2015). Inducible depletion of satellite cells in adult, sedentary mice impairs muscle regenerative capacity without affecting sarcopenia. *Nat Med* **21**, 76–80.
- Fry CS, Noehren B, Mula J, Ubele MF, Westgate PM, Kern PA & Peterson CA (2014b). Fibre type-specific satellite cell response to aerobic training in sedentary adults. *J Physiol* **592**, 2625–2635.
- Gosselin LE, Johnson BD & Sieck GC (1994). Age-related changes in diaphragm muscle contractile properties and myosin heavy chain isoforms. *Am J Resp Crit Care* **150**, 174–178.
- Greising SM, Mantilla CB, Gorman BA, Ermilov LG & Sieck GC (2013). Diaphragm muscle sarcopenia in aging mice. *Exp Gerontol* **48**, 881–887.
- Jackson JR, Kirby TJ, Fry CS, Cooper RL, McCarthy JJ, Peterson CA & Dupont-Versteegden EE (2015). Reduced voluntary running performance is associated with impaired coordination as a result of muscle satellite cell depletion in adult mice. *Skelet Muscle* **5**, 41.
- Jackson JR, Mula J, Kirby TJ, Fry CS, Lee JD, Ubele MF, Campbell KS, McCarthy JJ, Peterson CA & Dupont-Versteegden EE (2012). Satellite cell depletion does not inhibit adult skeletal muscle regrowth following unloading-induced atrophy. *Am J Physiol Cell Physiol* **303**, C854–C861.
- Keefe AC, Lawson JA, Flygare SD, Fox ZD, Colasanto MP, Mathew SJ, Yandell M & Kardon G (2015). Muscle stem cells contribute to myofibres in sedentary adult mice. *Nat Comm* **6**, 7087.
- Kirby TJ, Patel RM, McClintock TS, Dupont-Versteegden EE, Peterson CA & McCarthy JJ (2016). Myonuclear transcription is responsive to mechanical load and DNA content but uncoupled from cell size during hypertrophy. *Mol Biol Cell* **27**, 788–798.
- Kuang S, Chargé SB, Seale P, Huh M & Rudnicki MA (2006). Distinct roles for Pax7 and Pax3 in adult regenerative myogenesis. *J Cell Biol* **172**, 103–113.
- Lee JD, Fry CS, Mula J, Kirby TJ, Jackson JR, Liu F, Yang L, Dupont-Versteegden EE, McCarthy JJ & Peterson CA (2015). Aged muscle demonstrates fiber-type adaptations in response to mechanical overload, in the absence of myofiber hypertrophy, independent of satellite cell abundance. *J Gerontol Ser A Biol Sci Med Sci* **71**, 461–467.
- Lepper C, Partridge TA & Fan C-M (2011). An absolute requirement for Pax7-positive satellite cells in acute injury-induced skeletal muscle regeneration. *Development* **138**, 3639–3646.
- Liu W, Wei-LaPierre L, Klose A, Dirksen RT & Chakkalakal JV (2015). Inducible depletion of adult skeletal muscle stem cells impairs the regeneration of neuromuscular junctions. *eLife* **4**, e09221.
- Mackey AL, Kjaer M, Charifi N, Henriksson J, Bojsen-Moller J, Holm L & Kadi F (2009). Assessment of satellite cell number and activity status in human skeletal muscle biopsies. *Muscle Nerve* **40**, 455–465.
- McCarthy JJ, Mula J, Miyazaki M, Erfani R, Garrison K, Farooqui AB, Srikuea R, Lawson BA, Grimes B, Keller C, Van Zant G, Campbell KS, Esser KA, Dupont-Versteegden EE & Peterson CA (2011). Effective fiber hypertrophy in satellite cell-depleted skeletal muscle. *Development* **138**, 3657–3666.
- Montarras D, Morgan J, Collins C, Relaix F, Zaffran S, Cumano A, Partridge T & Buckingham M (2005). Direct isolation of satellite cells for skeletal muscle regeneration. *Science* **309**, 2064–2067.

- Moss F & Leblond C (1970). Nature of dividing nuclei in skeletal muscle of growing rats. *J Cell Biol* **44**, 459–461.
- Moss FP & Leblond CP (1971). Satellite cells as the source of nuclei in muscles of growing rats. *Anat Rec* **170**, 421–435.
- Murach KA, Walton RG, Fry CS, Michaelis SL, Groshong JS, Finlin BS, Kern PA & Peterson CA (2016). Cycle training modulates satellite cell and transcriptional responses to a bout of resistance exercise. *Physiol Rep* **4**, e12973.
- Murach KA, White SH, Wen Y, Ho A, Dupont-Versteegden EE, McCarthy JJ & Peterson CA (2017). Differential requirement for satellite cells during overload-induced muscle hypertrophy in growing versus mature mice. *Skelet Muscle* **7**, 14.
- Murphy MM, Lawson JA, Mathew SJ, Hutcheson DA & Kardon G (2011). Satellite cells, connective tissue fibroblasts and their interactions are crucial for muscle regeneration. *Development* **138**, 3625–3637.
- Pasut A & Rudnicki MA (2012). The long, the short, and the micro: a polyA tale of Pax3 in satellite cells. *Cell Stem Cell* **10**, 237–238.
- Pawlikowski B, Pulliam C, Betta ND, Kardon G & Olwin BB (2015). Pervasive satellite cell contribution to uninjured adult muscle fibers. *Skelet Muscle* **5**, 42.
- Polkey MI, Harris ML, Hughes PD, Hamnegard CH, Lyons D, Green M & Moxham J (1997). The contractile properties of the elderly human diaphragm. *Am J Resp Crit Care Med* **155**, 1560–1564.
- Relaix F, Montarras D, Zaffran S, Gayraud-Morel B, Rocancourt D, Tajbakhsh S, Mansouri A, Cumano A & Buckingham M (2006). Pax3 and Pax7 have distinct and overlapping functions in adult muscle progenitor cells. *J Cell Biol* **172**, 91–102.
- Sambasivan R, Yao R, Kissenpennig A, Van Wittenberghe L, Paldi A, Gayraud-Morel B, Guenou H, Malissen B, Tajbakhsh S & Galy A (2011). Pax7-expressing satellite cells are indispensable for adult skeletal muscle regeneration. *Development* **138**, 3647–3656.
- Schiaffino S, Bormioli SP & Aloisi M (1972). Cell proliferation in rat skeletal muscle during early stages of compensatory hypertrophy. *Virchows Archiv B Cell Pathol* **11**, 268–273.
- Shefer G, Van de Mark DP, Richardson JB & Yablonka-Reuveni Z (2006). Satellite-cell pool size does matter: defining the myogenic potency of aging skeletal muscle. *Dev Biol* **294**, 50–66.
- Snijders T, Verdijk LB & van Loon LJ (2009). The impact of sarcopenia and exercise training on skeletal muscle satellite cells. *Age Res Rev* **8**, 328–338.
- Southard S, Kim J-R, Low S, Tsika RW & Lepper C (2016). Myofiber-specific TEAD1 overexpression drives satellite cell hyperplasia and counters pathological effects of dystrophin deficiency. *eLife* **5**, e15461.
- Stockdale FE & Holtzer H (1961). DNA synthesis and myogenesis. *Exp Cell Res* **24**, 508–520.
- Tolep K, Higgins N, Muza S, Criner G & Kelsen SG (1995). Comparison of diaphragm strength between healthy adult elderly and young men. *Am J Resp Crit Care Med* **152**, 677–682.
- Tsukamoto K, Nakamura Y & Niikawa N (1994). Isolation of two isoforms of the PAX3 gene transcripts and their tissue-specific alternative expression in human adult tissues. *Human Gene* **93**, 270–274.
- Zimmerman SG, Peters NC, Altaras AE & Berg CA (2013). Optimized RNA ISH, RNA FISH and protein-RNA double labeling (IF/FISH) in Drosophila ovaries. *Nature Protoc* **8**, 2158–2179.

## Additional information

### Competing interests

The authors declare that they have no competing interests.

### Authors contributions

EDV conceived the study. CAP helped conceive the study. EDV participated in the study design. JRJ conducted experiments. ALC and LSG conducted experiments and analysis. EDV co-ordinated the data collection and analysis. KAM and AH conducted data analysis. KAM and ALC prepared figures. KAM drafted the manuscript. EDV helped draft the manuscript. ALC, AH, JRJ, LSG and CAP critically revised the manuscript. All authors approved the final version of the manuscript submitted for publication and agree to be accountable for all aspects of the work.

### Funding

This work was supported by grants from the National Institutes of Health to EDV (AG043721), KAM (AR071753) and CAP (AR060701).

### Acknowledgements

We thank Dr. John McCarthy, Alex Bugg, Parth Patel and Casey Potts for their technical assistance.